Mapping within-field variability of soybean evapotranspiration and crop coefficient using the Earth Engine Evaporation Flux (EEFlux) application

Luan Peroni Venancio[1]*, **Fernando Coelho Eugenio**[2], **Roberto Filgueiras**[1], **Fernando França da Cunha**[1], **Robson Argolo dos Santos**[1], **Wilian Rodrigues Ribeiro**[3], **Everardo Chartuni Mantovani**[1]

1 Department of Agricultural Engineering, Federal University of Viçosa, Viçosa, Minas Gerais, Brazil, **2** Department of Forest Engineering, Federal University of Santa Maria, Cachoeira do Sul, Rio Grande do Sul, Brazil, **3** Department of Rural Engineering, Federal University of Espírito Santo, Alegre, Espírito Santo, Brazil

* luan.venancio@ufv.br

Abstract

Accurate information about the spatiotemporal variability of actual crop evapotranspiration (ETa), crop coefficient (K_c) and water productivity (WP) is crucial for water efficient management in the agriculture. The Earth Engine Evapotranspiration Flux (EEFlux) application has become a popular approach for providing spatiotemporal information on ETa and Kc worldwide. The aim of this study was to quantify the variability of water consumption (ETa) and the K_c for an irrigated commercial planting of soybeans based on the EEFlux application in the western region of the state of Bahia, Brazil. The water productivity (WP) for the fields was also obtained. Six cloud-free images from Landsat 7 and 8 satellites, acquired during the 2016/17 soybean growing season were used and processed on the EEFlux platform. The ETa from EEFlux was compared to that of the modified FAO (MFAO) approach using the following statistical metrics: Willmot's index of agreement (d-*index*), root mean square error (RMSE), mean absolute error (MAE) and mean bias error (MBE). The K_c from EEFlux was compared to the K_c used in the soybean field (K_c FAO-based) and to the K_c values obtained in different scientific studies using the d-*index*. A similar procedure was performed for WP. Our results reveal that EEFlux is able to provide accurate information about the variability of ETa and the K_c of soybean fields. The comparison between ETa EEFlux and ETa MFAO showed good agreement based on the d-*index*, with values of 0.85, 0.83 and 0.89 for central pivots 1, 2 and 3, respectively. However, EEFlux tends to slightly underestimate ETa. The K_c EEFlux showed good accordance with the K_c values considered in this study, except in phase II, where a larger difference was observed; the average WP of the three fields (1.14 kg m^{-3}) was higher than that in the majority of the previous studies, which is a strong indicator of the efficient use of water in the studied soybean fields. The study showed that EEFlux, an innovative and free tool for access spatiotemporal variability of ETa and Kc at global scale is very efficient to estimate the ETa and Kc on different growth stages of soybean crop.

Competing interests: The authors have declared that no competing interests exist.

Introduction

One of the great current and future challenges worldwide is the production of more food to serve a growing population, which in 2050 can reach 9.73 billion people [1], in a scenario with less water available for agriculture. Thus, the appropriate management of water resources is extremely important [2]. In the specific case of irrigated agriculture, management is even more important because it represents the largest user of freshwater in the world, being responsible for approximately 70% of freshwater consumption, which is withdrawn from surface water and groundwater resources [1]. Among some of the reasons for the this high consumption, there is the low efficiency of the majority of the world existing irrigation systems, which is, on average, of only 56% [3], although there are systems with a higher irrigation efficiency, such as drip and central pivot. In addition, many irrigators do not adopt a method or tool monitor the crops water consumption. Zhang et al. [4] mentioned that, currently, irrigation depth is still often applied based on experience instead of science. To overcome this issue and consequently improve water use in agriculture, Kamali & Nazari [5] reported that two main strategies can be used: (i) upgrading operationally inefficient irrigation systems and (ii) improving irrigation planning and management.

With the current technological level of the irrigation industries, a lot of efficient equipment are available, so from an operational point of view, the first strategy can be relatively easy to reach. However, there a cost of acquisition and implantation of the system which need be carefully analyzed. The second point, however, is slightly more complex, as it is necessary to accurately quantify water consumption by crops, which, in turn, depends on the dynamic relationships between the soil-plant-atmosphere (SPA) system. The traditional ways to quantify the water consumption by crops are, mainly, the FAO (Food and Agriculture Organization) approaches (K_c single and dual) [6], weighing lysimeters, eddy-covariance (EC) systems and Bowen ratio [7]. These methodologies, although presenting many advantages, are locally based and, due to variations in climatic characteristics, have limitations when used on large areas [5]. In other words, these methodologies do not provide information on water consumption variability in the cultivation area. Thus, the location and quantity of the equipment (e.g., weather station, lysimeters and EC) must be strategic to have a reasonable representation of the whole area.

On the other hand, satellite-based surface energy balance models are a viable alternative to assess crop water consumption as well as to obtain K_c. Remote sensing (RS) has a strong advantage in spatial data acquisition since the information is acquired spatially [8] for large areas in a systematic way, with lower time and cost [5]. Mapping EvapoTranspiration at high Resolution using Internalized Calibration (METRIC) [9,10], which is capable of accurately estimating the water consumption by crops, has a very consistent physical basis and is one of the best models developed over the last few years; therefore, it has been successfully applied in many countries [8,11–13].

One of the problems related to the applicability of the energy balance models, targeted for final users, is the need for background knowledge in the physics of radiation [14,15]. METRIC users, for example, need to accumulate and assemble a variety of layers, including satellite images, land cover maps, terrain, local climate and soil maps from different sources and platforms, and there might be a significant amount of preprocessing required for the different layers before applying the algorithm [16]. Data entry and manipulation can be the most time-consuming phase of this process [17]. However, the Earth Engine Evapotranspiration Flux (EEFlux) platform has recently developed a METRIC version that operates on the Google Earth Engine (GEE) system [16,18]. Thus, the data entry and manipulation were automated, and the ET estimation process became faster than what was achieved with previous methods.

The goal of EEFlux development is the provision of on-demand estimates of the spatial distribution of water consumption by vegetation with 30 m spatial resolution, which are applicable to the 1984-present recording period for thermal-equipped Landsat imagery [19]. EEFlux also provides the rapid generation of intermediate products, such as surface temperature (Ts), normalized difference vegetation index (NDVI) [20] and albedo for a given Landsat scene, which may be useful for other applications besides ET [16]. EEFlux products can be considered "ready-to-use remote sensing products". Thus, this ease of use has motivated the scientific community to use these products instead of performing laborious imaging processing to generate similar products [15,21].

Some works have been conducted recently using EEFlux products [17,22–25]. Costa et al. [17] for example, found results satisfactory for estimate the spatial variability quantification of maize water consumption in Brazil [17]. Ayyad et al. [22], evaluated ETa from EEFlux in Egyptian agricultural areas of the Nile Delta and the Nile Valley and verified that their estimations produce overestimations for the ETa values. Khan et al. [23] compared ETa from EEFlux with eddy covariance measurements at four sites with five annual crops, and verified reasonable agreement between data. On the other hand, none of them has been carried out to soybean irrigated fields, and analyzed the variability of the crop evapotranspiration and crop coefficient, being our study the first. Study like the one being proposed is necessary to help in a better water use in agriculture, being also its important the knowledge about the water productivity (WP), a quantitative term used to define the relationship between agricultural output and the amount of freshwater involved in crop production (in kg m^{-3} or kg ha^{-1} mm^{-1}), which is a measure of the efficiency of water use [26,27].

Based on the importance of improving soybean irrigation planning and management, the present study aims to quantify the variability in water consumption (ETa) and the K_c for an irrigated commercial site of soybean planting based on the METRIC algorithm of the Google EEFlux application in the western region of the state of Bahia, Brazil. The specific objective includes a comparison of the spatial estimates of ETa EEFlux with the modified FAO method estimates, which is a verified and established method for crop evapotranspiration estimates in Brazil employed in the study area. In addition, we also aim to assess the water-use efficiency (WUE) in the soybean fields with the estimation of WP.

Materials and methods

Site description

The study was carried out on a traditional farm cropped with soybean (*Glycine max* L.) located in the municipality of São Desidério, in the western region of the state of Bahia, Brazil. Soybean is the main commercial oilseed crop and one of the main sources of vegetable oil and vegetable protein in the world [28,29] and is also the most important crop of Brazil [30]. This region stands out in the Brazilian and global map of agribusiness, being responsible to produces 100% of the soybean crop of the state, and 65% of its cultivated areas are occupied by this oilseed. In the 2017/18 harvest, the occupied area corresponded to 1.6 million hectares, with a production of 6.3 million tons and yield of 3.96 Mg ha^{-1} [31].Three central pivots with an area of 80 ha each were used. The central pivots were located in a rectangle, bound by the coordinate pairs 12˚26'45''S-45˚39'28''W and 12˚25'40''S-45˚37'48''W, and they had an average altitude of 750 m above sea level (Fig 1). According to Köppen's climatic classification [32], the climate of the region is tropical (Aw), with a rainy season in summer and dry winter, with an annual normal precipitation in the region of 1003.4 mm [33], concentrated in the rainy season (October to April). The region is characterized by having one of the highest concentrations of central pivots in Brazil [34] and being a great producer of cotton, soybean, and maize [35].
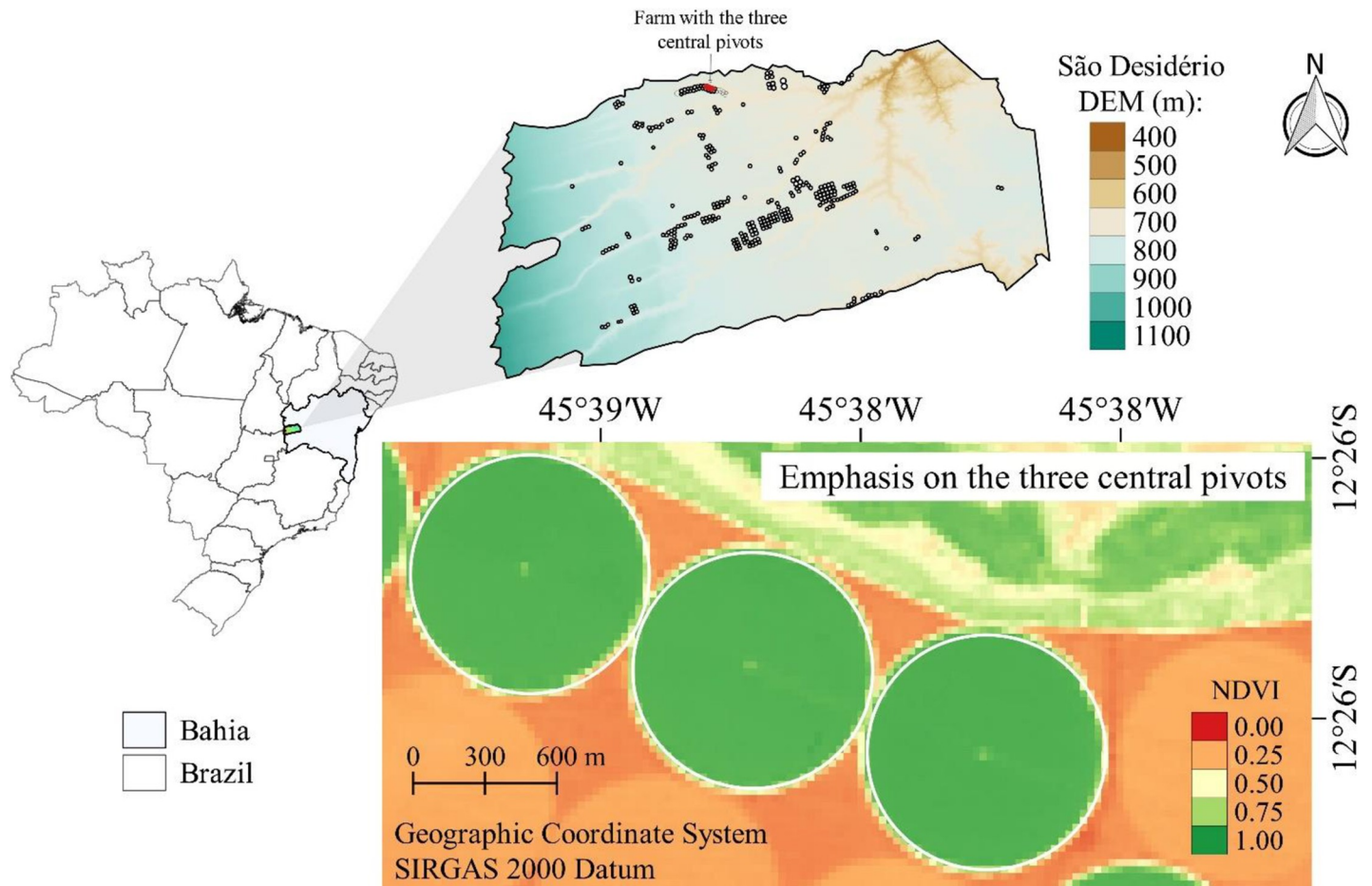
Fig 1. Location of study area and identification of the central pivots. DEM is the digital elevation model from the Shuttle Radar Topography Mission (SRTM) with a 30m spatial resolution downloaded from http://www.webmapit.com.br/inpe/topodata/. NDVI is the Normalized Difference Vegetation Index.

https://doi.org/10.1371/journal.pone.0235620.g001

Field data

Field data refer to the soybean (*Glycine max* L.) crop, meteorological conditions, and ETa collected during the 2016/2017 soybean growing season. The soybean data used in this study refer to the cultivar name, row and seed spacing, sowing and harvest date, cycle duration and yield mentioned in Table 1. Harvests were performed using harvesting machines, and the three central pivots were harvested together, which gave an average yield shown in Table 1.

Meteorological data acquired included minimum air temperature (Tmin, ˚C), maximum air temperature (Tmax, ˚C), wind speed at 2 m height (WS, m s^{-1}), radiation (Ra, MJ m^2 d^{-1}), relative humidity (RH, %) and rainfall (mm). These data were obtained from an automatic meteorological station located near the central pivots. The soybean ETa was also measured, calculated using the modified FAO method (MFAO) [36,37]. The temporal variations in these meteorological data over the season are presented in the results and discussion.

Table 1. Data referring to the soybean (*Glycine max* L.) cropped in the central pivots 1, 2 and 3 in the crop season 2016/2017.

Cultivar -	Spacing (seeds × row)	Sowing date -	Harvest date -	Cycle (days)	Yield (kg ha^{-1})
Monsoy—M8349 IPRO	0.2 × 0.45 m	24/10/2016	04/03/2017	131	4,042

https://doi.org/10.1371/journal.pone.0235620.t001

Actual crop evapotranspiration (ETa) estimates

Modified FAO method. Soybean ETa was estimated by the modified FAO method (MFAO), an approach verified in Brazil in large irrigated commercial areas and abroad, through the irrigation platform "IRRIGER Connect" from Valmont Industries [38]. This methodology is also largely applied in scientific research [39–41]. The MFAO method is derived from the single-crop coefficient empirical method (Allen et al., 1998; Doorenbos and Pruitt, 1977), which is one of the most commonly used methods for irrigation water management [42,43] (Eq 1).

$$ETa = ETo \times K_c \times K_S \times K_L \tag{1}$$

where ETa is the actual crop evapotranspiration (mm d^{-1}), ETo is the grass reference evapotranspiration according to the FAO Penman-Monteith method approach [6] (mm d^{-1}), K_c is the crop coefficient, K_S is the water stress coefficient [37,40] and K_L is the localized water application coefficient [44]. The value of K_L is 1 when the whole cultivated area is wetted by an irrigation system (e.g., areas are irrigated by central pivots).

The K_c values used in the MFAO method for soybean ETa determination are derived from the values recommended by the FAO-56 approach [6]. Table 2 shows the following K_c values based on the grass-reference evapotranspiration used.

The K_S is used to incorporate the water stress effect on reducing crop transpiration, and the daily K_S estimation in the root zone [37] is computed as follows (Eq 2):

$$K_S = \frac{\ln(1 + CSWS)}{\ln(1 + SWS)} \tag{2}$$

where SWS is the total soil water storage (mm) and CSWS is the current soil water storage (mm).

Earth Engine Evapotranspiration Flux (EEFlux). The Earth Engine Evapotranspiration Flux (EEFlux) is patterned after the operational stand-alone METRIC (Mapping Evapotranspiration at High Resolution with Internal Calibration) model [9,10]. EEFlux is a full surface energy balance model that produces estimates of net radiation (Rn), sensible heat flux (H) and soil heat flux (G) [16,18]. The ETa is estimated as a residual of the surface energy balance [9,10], according to Eq 3.

$$LE = Rn - H - G \tag{3}$$

where LE is the latent heat flux—spent energy in the evapotranspiration process (W m^{-2}), Rn is the net radiation (W m^{-2}), G is the soil heat flux, (W m^{-2}) and H is the sensible heat flux (W m^{-2}).

Table 2. Information about soybean K_c used in the MFAO method for ETa estimates.

FAO phenological phase	Phenological phase No.	K_c value	Length (days)	K_c calculation
Initial	I	0.35	15	Constant
Development	II	-	35	Linear interpolation
Mid-season	III	1.00	52	Constant
Late-season	IV	-	30	Linear interpolation
End	-	0.70	-	Constant

Kc during the crop development phase: linear interpolation between Kc values of the I and III phenological phases. Kc during the late-season phase: linear interpolation between Kc values of the III and Kc end.

The LE is estimated at the exact satellite overpass time for each pixel. The ETa is then calculated by dividing LE by the latent heat of vaporization, according to Eq 4.

$$ET_{inst} = \frac{LE}{\lambda \rho_w} \times 3600 \tag{4}$$

where ET_{inst} is the instant evapotranspiration (mm h^{-1}), 3600 converts seconds to hours, λ is the latent heat of vaporization (J kg^{-1}) and ρ_w is the density of water ($\sim$ kg 1000 m^{-3}).

Later, the fraction of the reference evapotranspiration (ETrF) was calculated for each pixel by the ratio of the computed ETinst to the instantaneous alfalfa reference evapotranspiration (ETr), according to Eq 5, and it was used as a vehicle to extrapolate ET from the instantaneous passage of the satellite to a 24-h period. The ETrF is a crop coefficient relative to ETr (K_{cr}) since alfalfa is the reference crop adopted in METRIC [45].

$$ET_rF = \frac{ET_{ins}}{ET_r} \tag{5}$$

Thus, the daily ETa is estimated by multiplying ETrF values for each individual pixel by daily ETr, computed from local or gridded weather data, assuming consistency between the ETrF at the time of the satellite passage and the ETrF for the 24-hour period, as follows.

$$ET_a = ET_{inst} \times ET_rF \tag{6}$$

It is important to note that both EEFlux and METRIC applications utilize the alfalfa reference evapotranspiration (ETr) [46] instead of the ETo to estimate the daily ETa [16]. However, in the central pivots of this study, the ETo was used instead of the ETr to estimate the ETa. Thus, part of the difference between the estimates (EEFlux and MFAO) that will be verified can be attributed to this, although the difference between the derived ETa to ETr or ETo can be considered small, due to K_c value adjustments [6].

To quantify the variability of ETa and K_c, six Landsat 7 and 8 satellite images were used and processed on Earth Engine Evapotranspiration Flux (EEFlux/METRIC version 0.20.2; https://eeflux-level1.appspot.com/). Table 3 shows the Landsat 7 and 8 image information, as well as information related to the soybean crop: days after sowing (DAS) and soybean growth stages for the image dates. In addition, Table 4 shows details of the agrometeorological conditions on the date of the images collections.

Crop coefficient (K_c)

The K_c derived from EEFlux, which is an alfalfa-based crop coefficient, was compared to the K_c adopted in soybean fields (FAO-based Kc) and with those derived from studies performed

Table 3. Details for Landsat satellite used (7 or 8), date and Day of The Year (DOY) of acquisition of the image, Days After Sowing (DAS), soybean growth stages and FAO phenological stage of soybean (*Glycine max* L.), considering Monsoy—M8349 IPRO cultivar growth.

Landsat	Acquisition		DAS	Soybean growth stages	FAO phenological stage
	Date	DOY			
7	Oct. 26, 2016	300	002	VE—Emergence	I—Initial
8	Nov. 03, 2016	308	010	V1—First trifoliolate	I—Initial
8	Jan. 06, 2017	006	074	R4—Full pod	II—Development
8	Jan. 22, 2017	022	090	R5—Beginning seed	III—Mid-season
7	Feb. 15, 2017	046	114	R6—Full seed	IV—Late-season
8	Feb. 23, 2017	054	122	R7—Beginning maturity	IV—Late-season

Table 4. Agrometeorological conditions on the date of the images collections.

Acquisition date	Tm (°C)	RH (%)	WS (m s^{-1})	Ra (MJ m^{-2} d^{-1})	P (mm)	ETo (mm d^{-1})
Oct. 26, 2016	26.8	50.0	2.1	30.6	0.0	6.8
Nov. 03, 2016	27.3	39.0	3.4	31.8	0.0	8.4
Jan. 06, 2017	27.6	49.7	0.3	26.9	0.0	4.8
Jan. 22, 2017	25.5	70.4	2.2	29.4	0.0	5.9
Feb. 15, 2017	22.7	79.1	1.8	21.4	0.0	3.8
Feb. 23, 2017	24.7	71.3	1.7	29.2	0.0	5.4

Tm—mean air temperature. RH—relative humidity. WS—wind speed at 2 m height. Ra—extraterrestrial radiation. P—rainfall. ETo—grass reference evapotranspiration.

https://doi.org/10.1371/journal.pone.0235620.t004

in the United States and Brazil. Those K_c values obtained based on grass were converted into alfalfa-based K_c through the means of their division by a conversion factor (K_{ratio}) calculated using Eq 7, as recommended in the FAO 56 approach [6].

$$K_{ratio} = 1.2\left[0.04\,(WS - 2) - 0.04\,(RH_{min} - 45)\left(\frac{h}{3}\right)\right] \tag{7}$$

where WS is the wind speed at 2 m height (m s^{-1}), RH_{min} is the relative humidity (%) and h is equal to 0.5, which is the standard height for the alfalfa reference.

In addition, the K_c values were strategically chosen to coincide with the image date or near to it, allowing their comparison with K_c EEFlux. The K_c values after conversion to the alfalfa reference are presented in Table 5.

Water productivity (WP) and NDVI-K_c relationship

The WP, also denominated as water use efficiency (WUE), is a quantitative term used to define the relationship between agricultural output and the amount of freshwater involved in crop production (in kg m^{-3} or kg ha^{-1} mm^{-1}) [26,27,50]. Crop WP in this study was expressed in terms of actual evapotranspiration (WP$_{ETa}$) according to Eq 8 [27].

$$WP = \frac{Ys}{\sum ET_a} \tag{8}$$

where WP is the water productivity (kg ha^{-1} mm^{-1} or kg m^{-3}), Ys is the soybean yield (kg ha^{-1}) and ΣETa is the sum of ETa over the season calculated by the MFAO method (mm or m^3 ha^{-1}).

Table 5. Soybean crop coefficient (K_c) based on alfalfa reference evapotranspiration obtained in different phenological stages established by the FAO (I—initial; II—development; III—mid-season; and IV—late-season) along with the respective days after sowing (DAS), calculated in irrigated areas by central pivots in the United States and Brazil.

Reference—Region	K_c values (Approximate DAS)				
	I	II	III	IV-1	IV-2
Allen et al. [6]—USA[a]	0.29 (002)	0.83 (074)	0.83 (090)	0.72 (114)	0.61 (122)
Singh & Irmak [47]—USA[b]	0.24 (004)	0.86 (068)	1.11 (084)	0.75 (116)	0.58 (124)
Suyker & Verma [48]–USA	0.17 (010)	0.79 (075)	0.91 (090)	0.62 (110)	0.25 (120)
Monteiro & Sentelhas [49]—BRA[c]	0.25 (001)	0.62 (064)	0.95 (093)	0.66 (110)	0.66 (120)

[a] Kc adopted in the soybean fields after their conversion to alfalfa-based Kc.

[b] Kc derived from alfalfa-reference evapotranspiration (ETr), so conversion was not necessary.

[c] the work does not specify whether the areas were irrigated.

https://doi.org/10.1371/journal.pone.0235620.t005

The relationship between NDVI and the Kc, named NDVI-Kc relationship, was establish by means a simple linear regression. NDVI was chosen because, similar to ETa and K_c, it is available "ready-to-use" in the EEFlux platform. Furthermore, the NDVI is probably the most frequently used vegetation index for crop biophysical parameter access. Eq 9 and the K_c are both derived from the EEFlux platform.

$$\mathrm{NDVI} = \frac{(\rho_{\mathrm{NIR}} - \rho_{\mathrm{red}})}{(\rho_{\mathrm{NIR}} + \rho_{\mathrm{red}})} \tag{9}$$

where ρ_{NIR} and ρ_{red} refer to the reflectance of the near-infrared and red spectral bands, respectively.

Variables, maps, and statistical analysis

The temporal and spatial dynamics of ETa and K_c have been developed. In addition, the temporal and spatial distribution of NDVI was obtained to assess soybean development over the season. Then, the descriptive statistical (i.e., average, minimum and maximum values) sample was obtained by a boxplot for the NDVI, ETa and K_c based on EEFlux data for each of the seven Landsat images acquired over the season. Later, the ETa obtained through EEFlux was compared to the ETa observed in the field (MFAO) using the following statistical metrics: Willmot's index of agreement (d-*index*) [51], root mean square error (RMSE), mean absolute error (MAE) and mean bias error (MBE). The K_c was compared using only the d-*index*. The d-*index* value of 1 indicates a perfect match, and 0 indicates no agreement at all.

Results and discussion

Climatic conditions and irrigation depth

The seasonal meteorological data during the 2016/17 soybean growing season are presented in Fig 2. The average air temperature over the crop season was 24.8˚C, with maximum and minimum temperatures of 28.4 and 21.0˚C, respectively. The average temperature remained slightly below that of the climatological normal for the region, which in this period of the year is 25.98˚C [33]. The highest temperatures and the highest irrigation demand (high evapotranspiration) corresponded to the summer months (December to March), which also experienced considerable rainfall events.

In relation to rainfall, during the 2016/17 soybean season (Oct. 24, 2016, to March 04, 2017), there were 38 rain events, totalizing 445 mm (Fig 2); consequently, irrigation is predicated as a supplementary practice in this period, which is different for the winter plantings when the full cycle is irrigated. The irrigation was performed only 14 times, with a total irrigation depth applied of 103.1 mm. (Fig 2.). The ETo had an average value of 4.65 mm d^{-1} with some peaks in early and late November, which reached values higher than 8 mm. Much attention must be given when this high ETo peak occurs to avoid deficient irrigation depth that can, as a consequence, cause water stress in the plants. For example, stress during node emergence delays node appearance and hastens the formation of reproductive organs on these nodes, while if the plants are subjected to stress during flower and pod formation, they have a shorter period in which organs appear [52].

As the EEFlux is an energy balance-based model [16,18], the climatic conditions have a lot influence on their analysis, specially the solar radiation variable, main component of energy balance. Another point is that EEFlux requires identification of a hot and cold pixels in the image, thus, in the wet season or in irrigated areas the hot pixel can be hard to be identify, leading to inconsistent results. However, according to o Floolad et al. [16], in the EEFlux, these
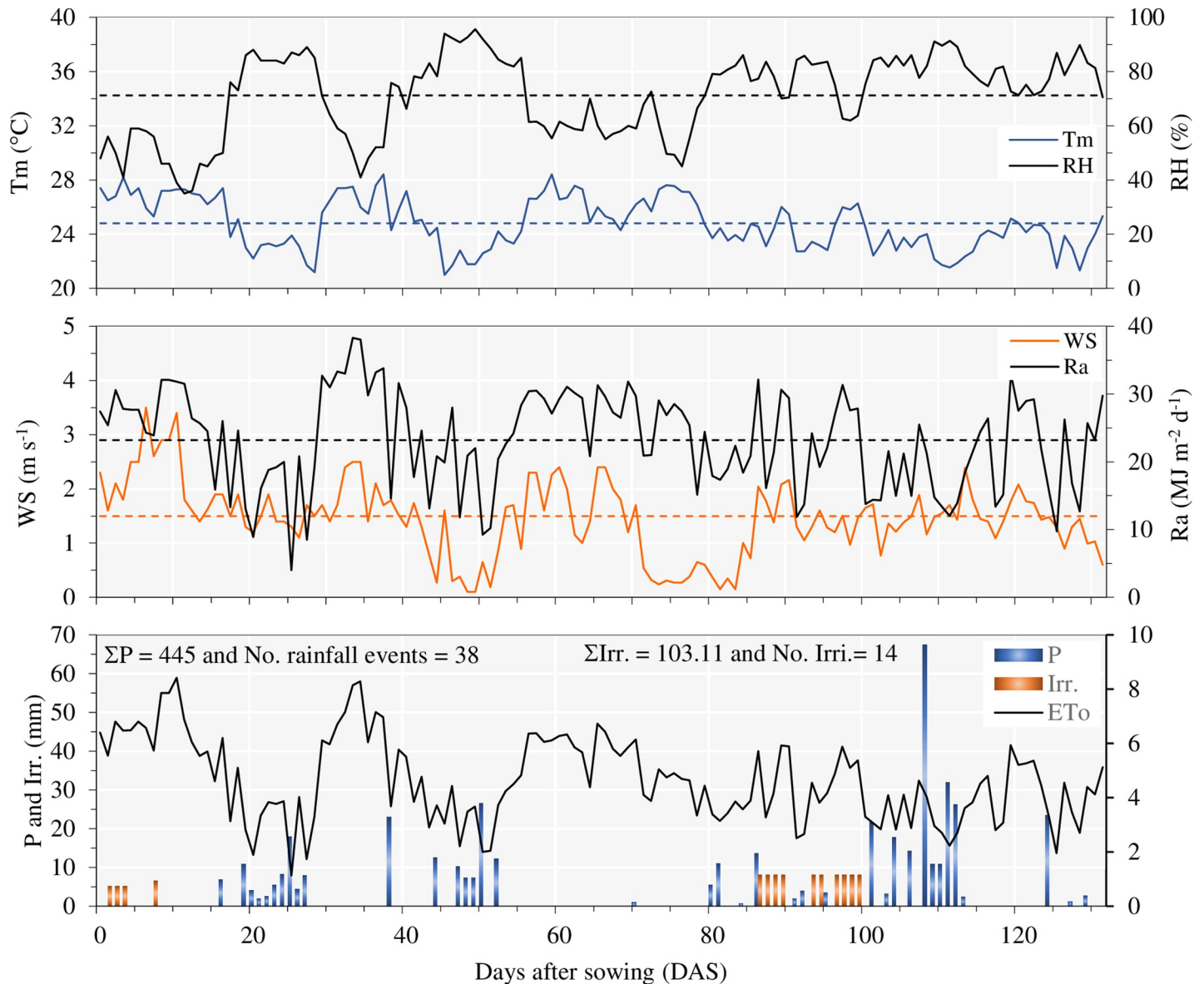
Fig 2. Meteorological data during the soybean growing season 2016/17. Tm: mean air temperature; RH: relative humidity; WS: wind speed at 2 m height; Ra: extraterrestrial radiation; P: rainfall; ETo: grass reference evapotranspiration; Irr.: irrigation depth. The dashed line represents the average of the data in the season.

pixels are determined automatically with a great effectiveness in agricultural areas, generating ETrF and ETa values comparable to the values from trained expert to choose these pixels.

Within-field variability of NDVI, ETa and Kc

Understanding patterns of vegetation based on spectral vegetation indices (VI) is essential for crop management and to help farmers make decisions [40]. Fig 3A shows the spatiotemporal distribution of NDVI over the soybean growing season. As expected for normal soybean cultivation, low NDVI values were found in the initial stages (0 and 010 DAS) due to the larger amount of uncovered soil in this period. The emergence of soybeans usually occurs 5 to 10 days after sowing, depending on moisture and temperature conditions [53,54]. According to
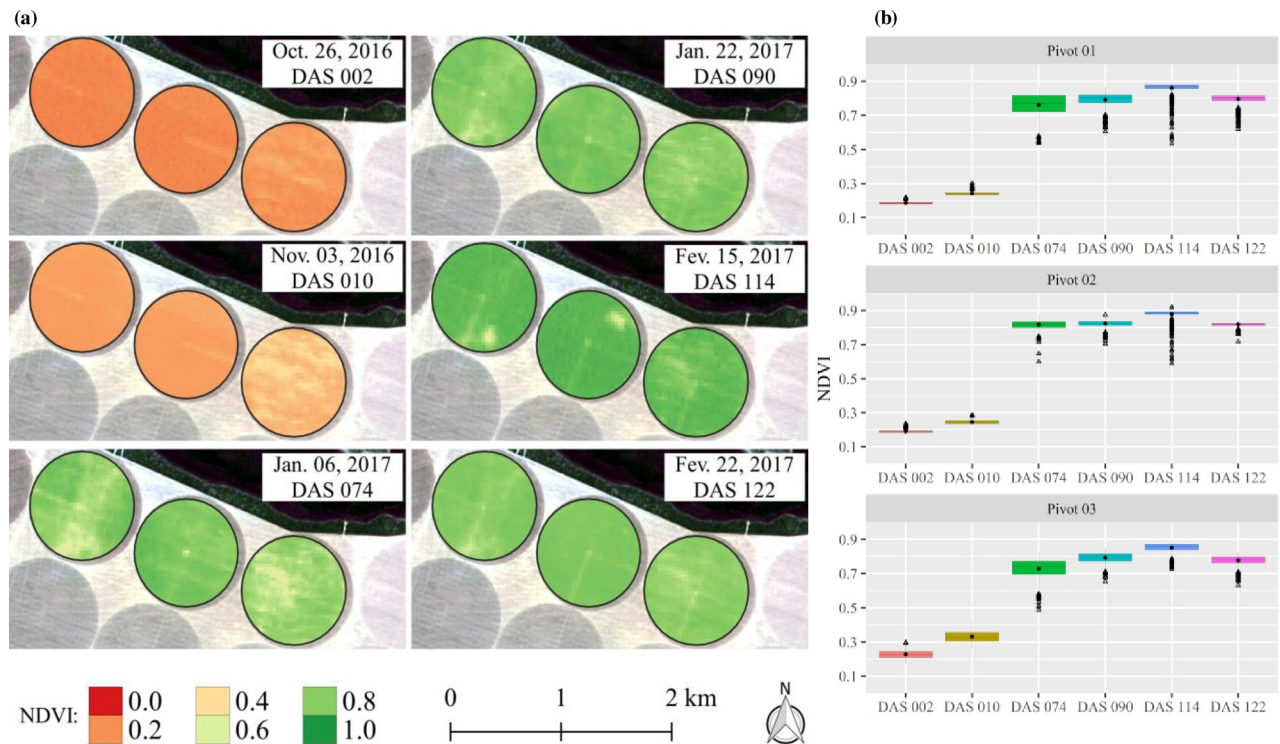
Fig 3. Spatiotemporal distribution (a) and boxplot (b) of the normalized difference vegetation index (NDVI) as a function of days after sowing (DAS) in the 2016/17 soybean growing season.

https://doi.org/10.1371/journal.pone.0235620.g003

González-Gómez et al. [55], during the crop implantation phase, the vegetation index responses are mainly attributable to the bare soil or the remaining previous crop in direct sowing fields.

An expressive increase in NDVI during the development phase was verified, which can be clearly attested to by the difference between images at 010 and 074 DAS (Fig 3A and 3B). During the mid-season (074 and 090 DAS) and initial part of the late season (144 DAS), a low variability in the values was observed, and in the final portion of the late season (122 DAS) (Fig 3A), a reduction in the NDVI values until physiological maturity due to plant senescence was noticed [53]. It is important to note that this soybean cultivar (Monsoy—M8349 IPRO) presents a cycle of approximately 140 days in the study region; thus, at 122 DAS, the soybean still presents a high NDVI value (approximately 0.8) (Fig 3B). However, from this time, NDVI tends to decrease very fast until the R8 stage, where full maturity is reached– 95% of the pods have reached their mature pod color [53,54].

With 074 DAS, zones with low NDVI values were identified in central pivots 1 and 3, while in central pivot 2, we observed a great uniformity in NDVI values, that is, low data variability. The explanations for this are soil patches and failures in fertilization applications, since pests and diseases in the fields were not observed. On the other hand, in the last three images, a significant variability in NDVI values was not found. NDVI values during the season ranged from 0.2 to 0.9 (Fig 3A), which is a very common variation in soybean fields [56–59], with average rates always higher than 0.7 in the development, mid-season and late-season phenological phases. The small amplitudes of the boxplots reveal that vegetation conditions were slightly variable between the three fields over the growing season. This is a consequence of the high technological level adopted on the farm and of the use of only one cultivar.
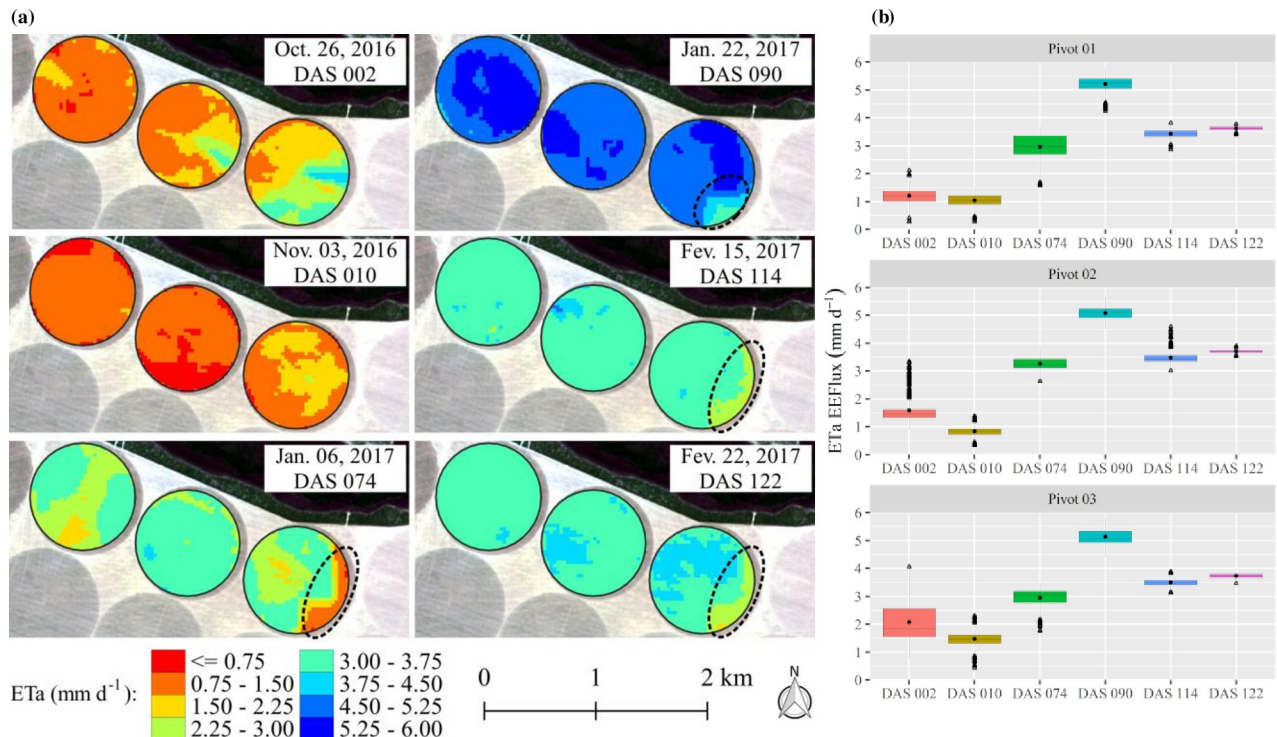
Fig 4. Spatiotemporal distribution (a) and boxplot (b) of the soybean actual evapotranspiration (ETa) values as a function of the days after sowing (DAS) in the 2016/17 soybean growing season. The area inside of the dashed line refers to the part considered affected.

https://doi.org/10.1371/journal.pone.0235620.g004

The spatial and temporal variability of the soybean ETa from EEFlux over fields are presented in Fig 4A. In the first image (002 DAS), the major variability among the six images considered was verified, highlighting pivot 3 with two well-distinct zones, which can also be attested to with the boxplot amplitude. The two zones are a consequence of irrigation in a slice of the central pivot (east zone). Similar results were verified for central pivot number 2. The higher ETa value is verified at 090 DAS and is highly influenced by the high leaf area index, which normally has a maximum value at approximately 80 DAS [60,61]. The ETa remained relatively high in the subsequent images (114 and 122 DAS), and with respect to ETa uniformity, the greatest uniformities were observed in the three last images as a consequence of the good crop establishment in the area.

The boxplot of ETa values for the central pivots cultivated in the 2016/17 growing season are shown in Fig 4B. The average ETa values ranged from 1 to 5 mm d^{-1} considering the three fields. In addition to the NDVI, the ETa presented a seasonal behavior very characteristic of annual crops, that is, low values at the start of the crop season, maximum values in the mid-season and decreased values in the late season. The detection of within-field variability by satellite or remotely piloted aircraft system (RPAS) images can be very useful for precision irrigation because this approach can provide specific information about irrigation, such as water application uniformity, areas with irrigation deficits or surface runoff areas near the outer boundary of the central pivot systems. For Campos et al. [62], the variable application of agronomic inputs (e.g., water using variable-rate irrigation by central pivot) is an obstacle to precision agriculture, and variability maps can be essential for overcoming these obstacles because they provide accurate information about the real demand of each field zone.

It is important to note that the ETa and ETrF EEFlux products presented inconsistency in some parts of pivot 3 (area within the dashed line, Figs 4A and 5A); specifically, patches of
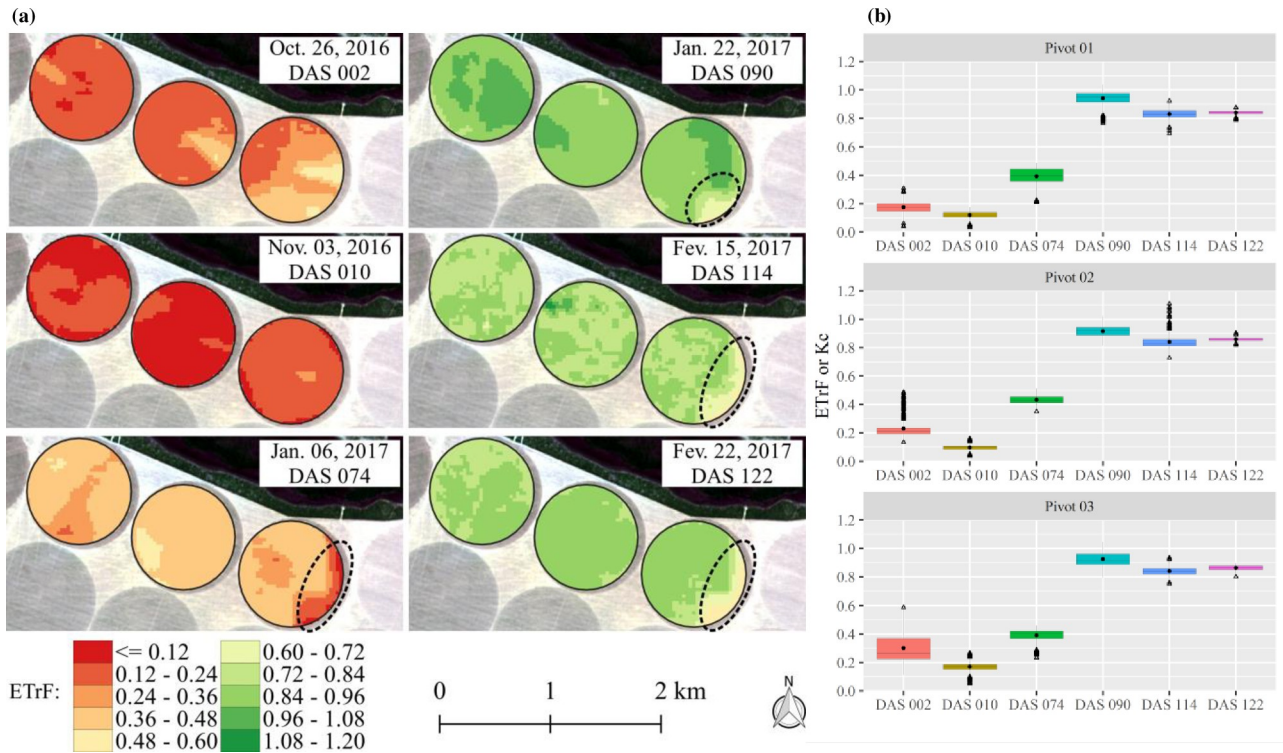
Fig 5. Spatiotemporal distribution (a) and boxplot (b) of the fraction of the reference evapotranspiration (ETrF) or alfalfa-based crop coefficient (K_c) values as a function of the days after sowing (DAS) in the 2016/17 soybean growing season. The area inside of the dashed line refers to the part considered affected.

known geometry appeared—a kind of oversize pixel—very different from the Landsat 30 m-pixel (S1–S3 Figs). In addition, low values were verified in these areas when compared to the non-affected zones. A specific answer to this issue was not found in the literature, but it strongly looks like a simple processing error of the gridded weather data required for their calibration and calculation (e.g., of the ETa and ETrF), which show very low spatial resolution. In the present study area and in all other areas outside of the continuous United States, EEFlux uses Climate Forecast System Version 2 (CFSv2) and the Climate Forecast System Reanalysis (CFSR) gridded weather data for all calculations [16]. Another point that supports this hypothesis is that NDVI images, which do not require these climatic data, do not present the same issue. These affected zones were not considered in the statistical analyses.

The spatiotemporal evolution of the K_c for the three central pivots with soybeans followed a well-defined pattern featuring four different phases, such as crop implantation, fast growth, peak, and decrease, as also defined in FAO 56 (Fig 5A and 5B). It is verified that K_c ranged from approximately 0.10 to 1.0 considering mean values and all center pivots (Fig 5B) and, as expected, the highest values occurred in the mid-season (in this case, 090 DAS), when the soybeans have a maximum leaf area index and a higher vigor, as previously referenced. This K_c amplitude follows the findings presented by Kamble et al. [63]. An important detail (also occurring in ETa) is that the K_c value at 010 DAS is lower than 002. The most important reason for these results was the irrigation performed in the two first-day cycles (commonly called "irrigation for germination"), which made the soil more moist and consequently increased the K_c EEFlux, while in the two days previous to 010 DAS, the water (rain or irrigation) was not applied. Overall, the K_c presented a good spatial distribution pattern, which was close to the
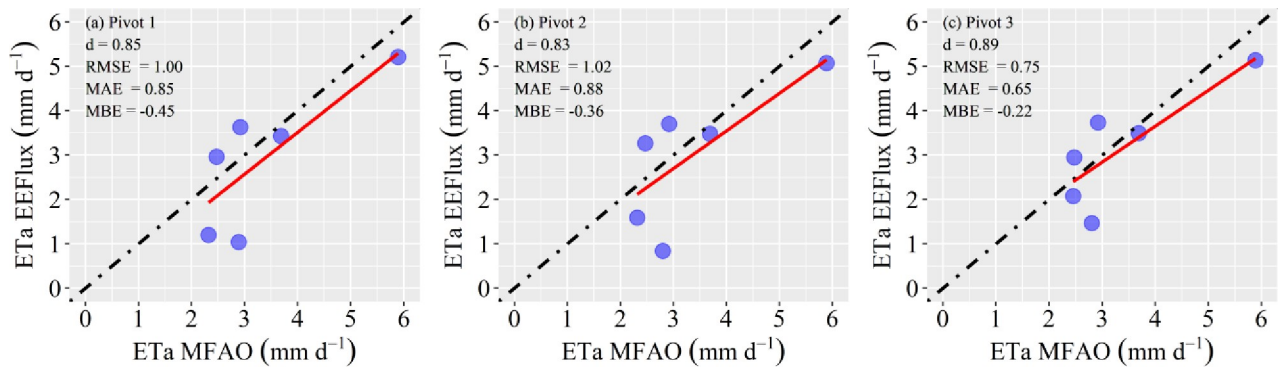
Fig 6. Comparison scatterplot between the average daily ETa from the MFAO approach and the ETa estimated by the EEFlux algorithm across the three central pivots in the 2016/17 soybean growing season. The dot-dashed line represents the 1:1 line, and the solid red line represents the linear regression.

https://doi.org/10.1371/journal.pone.0235620.g006

pattern found for ETa. This good spatial pattern as well as the convenient K_c values enables the combination with a traditional irrigation management system, such as the MFAO and FAO 56 approaches.

Comparison of the ETa and Kc EEFlux with the MFAO

The scatterplots in Fig 6 show comparisons between the average daily ETa from the MFAO approach and the ETa estimated by the EEFlux algorithm across the three central pivots in the 2016/17 soybean growing season. The corresponding values for the d-*index* were 0.85, 0.83 and 0.89 for pivots 1, 2 and 3, respectively, indicating a very good correlation between the ETa MFAO and ETa EEFlux. On the other hand, taking into account the RMSE, the difference between ETa EEFlux and MFAO was large in pivots 1 and 2, with values close to 1.0 and slightly smaller in pivot 3 (0.75 mm d^{-1}). MAE was also higher for pivots 1 and 2 than that in field 3. It can also be deduced from MBE (Fig 6) that EEFlux tends to underestimate the ETa, especially when MFAO presents low(er) ETa values, as occurs in the initial phenological phases.

Overall, the comparison (using MFAO as reference) results were very satisfactory once MFAO data were updated and EEFlux incorporated the variability in the fields. A second point can be related to the use of an average Kc value in the MFAO during the initial and mid-season phases [6], while EEFlux, as well as other evapotranspiration models, takes into account the current conditions at the satellite overpass time. Another point is that the MFAO evapotranspiration was based on grass reference evapotranspiration, while EEFlux was calculated using the alfalfa reference, which can also contribute to the difference that was verified. Last, there are also limitations related to the number of samples available within the crop cycle, where the small number of samples tends to decrease the precision and accuracy of ET estimation models [17].

The comparison among the average values of the soybean K_c derived from EEFlux with the K_c adopted in the soybean fields and those derived from studies performed in the United States and Brazil are presented in Fig 7. The K_{ratio} value obtained to convert Kc-grass into Kc-alfalfa was 1.21, which is very close to the value recommended for semiarid regions, which is 1.20 [6]. First, it is important to highlight that K_c EEFlux agrees very well with the crop-development phases; that is, there are lower values during the initial period (phase I), a substantial increase in phase II in comparison to that of the previous phase, maximum values reached in mid-season (phase III) and a decrease in values in the last phase (IV). The average K_c EEFlux values
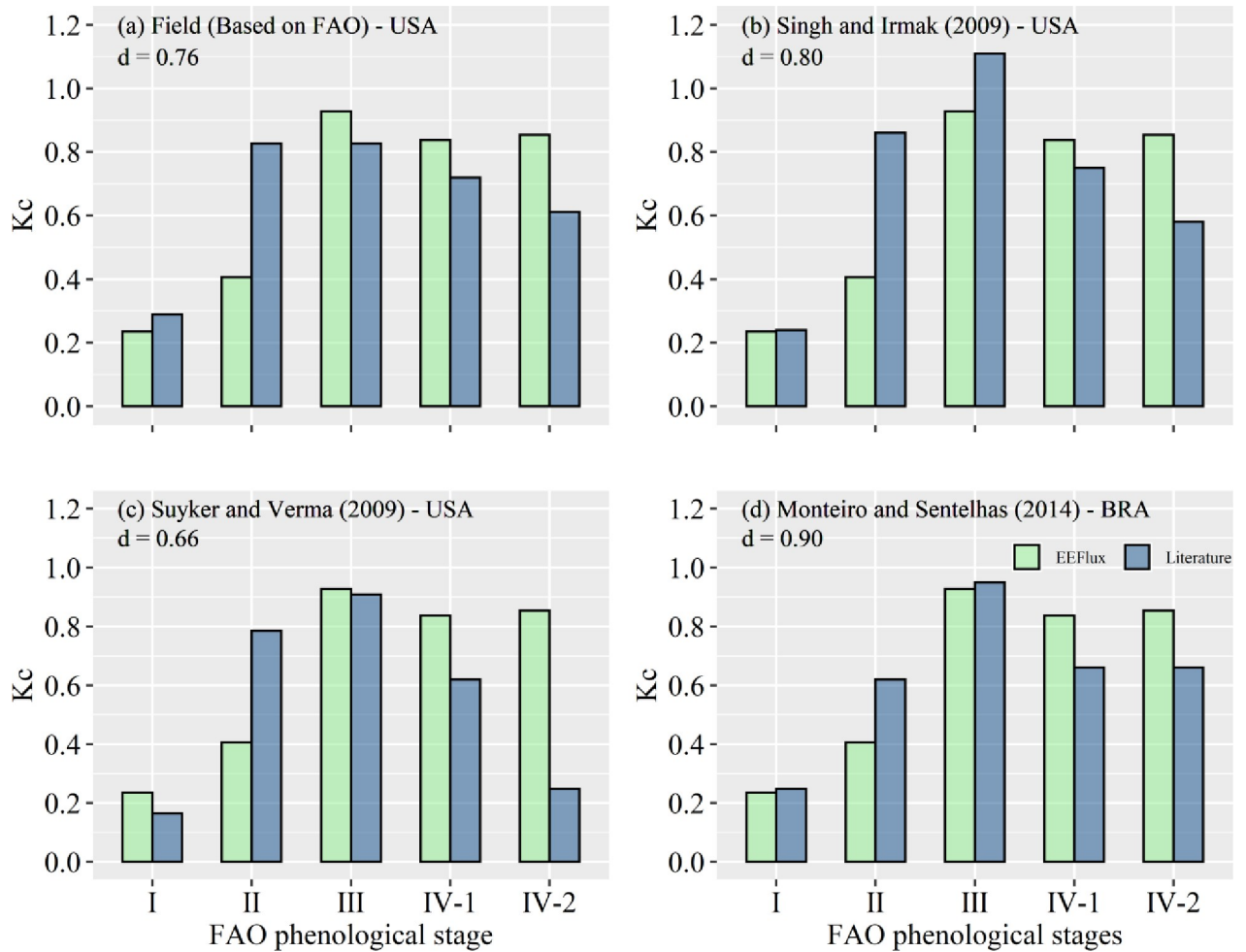
Fig 7. Soybean crop coefficient (K_c) derived from EEFlux compared with the K_c adopted in the soybean fields and with those derived from studies performed in the United States and Brazil. The numbers 1 and 2 after phase IV indicate that the two images were acquired within this phase (see Table 5).

obtained from soybean were 0.24, 0.41, 0.93, 0.84 and 0.85 for I, II, III, IV-1 and IV-2, respectively.

The comparison between K_c EEFlux and K_c used in the soybean fields, which is based on those values presented in the FAO 56 bulletin [6] can be observed in Fig 7A. There were verified close values for phases I, III, IV-1 and IV-2 and a higher difference in phase II, where K_c FAO values were two times higher than those of K_c EEFlux. Similar results were verified for the comparison with Singh & Irmak [47] data (Fig 7B) and Suyker & Verma [48] (Fig 7C). In addition to presenting a large difference in phase II, the results of Suyker & Verma [48] also showed a large difference in phase IV-2. The comparison of the K_c EEFlux to the K_c determined by Monteiro & Sentelhas [49] showed the best agreements (d = 0.90) (Fig 7D) and also showed a lower K_c difference in phase II, which did not occur in the other comparisons.

Costa et al. [17], in a very similar study, compared K_c EEFlux to K_c derived from FAO56 for maize crops, and according to them, the difference between K_c values is related to the temporal variability. Once the K_c FAO is obtained from multiday data, the K_c EEFlux is obtained from the passing time data of the satellite, which makes these methodologies considerably different. Another two points to be considered are the edaphoclimatic conditions and the methodologies
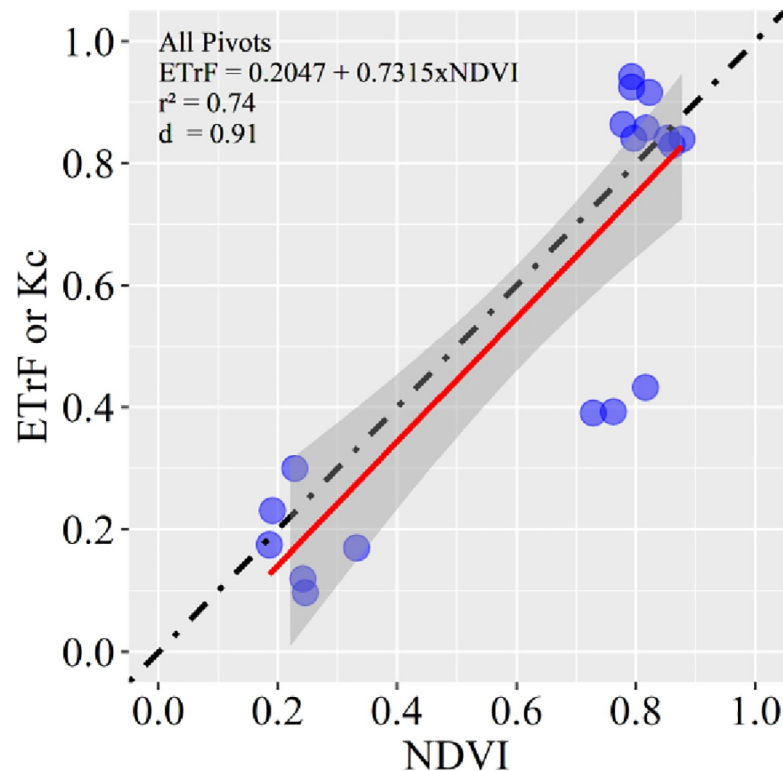
Fig 8. Linear relationship between NDVI and ETrF or K_c using data of all three central pivots with soybeans in the 2016/17 growing season. The smoothed area represents the 95% confidence interval. The dot-dashed line represents the 1:1 line, and the solid red line represents the linear regression.

https://doi.org/10.1371/journal.pone.0235620.g008

used to obtain the K_c, which possibly are different from those in the current study (satellite data with 30 m spatial resolution). Overall, K_c EEFlux represented soybean development well, which makes these products an important possibility for precision irrigation practices.

NDVI-K_c relationship

The relationship between NDVI and K_c for irrigated soybean crops in the 2016/17 growing season is shown in Fig 8. There was a good correlation between NDVI and the K_c, with a coefficient of determination (r^2) equal to 0.74, which is very informative regarding the amount of variance that NDVI can explain in the K_c dataset. The d-*index* is 0.91, which means there is very good agreement between the datasets. An interest in estimating the K_c with the vegetation index, mainly to generate information for irrigation scheduling, appears with the availability of high spatial and temporal resolution multispectral satellite systems and the emergence of ultrahigh spatial resolution aerial platforms such as RPAS [64]. This fact would help precision irrigation practices, especially at a regional scale.

The isolated group with three NDVI values of approximately 0.8 and K_c of 0.4 is related to the image corresponding to 074 DAS (Figs 3B and 5B), where NDVI (depending only on vegetation) is high (≈ 0.8), while ETrF, which depends on more factors (e.g., soil moisture and climatic conditions), remained at approximately 0.4. One of the first works developed with this objective was performed by Bausch and Neale [65], and since then, numerous studies have found good results in estimating vegetation index-based K_c using linear regression models in different agricultural areas around the world [63,64,66,67].

Table 6. Water productivity (WP) for the central pivots in the 2016/17 soybean growing season.

Central Pivot	Sum ETa MFAO (mm)	Sum ETa MFAO (m^3 ha^{-1})	Yield (kg ha^{-1})	WP (kg ha^{-1} mm^{-1})	WP (kg m^{-3})
1	361.5	3,615.4	4,042	11.18	1.12
2	360.9	3,609.4	4,042	11.20	1.12
3	344.3	3,443.0	4,042	11.74	1.17
Mean	355.6	3,555.9	4,042	11.37	1.14

Soybean WP

Table 6 shows the soybean water productivity (WP) on two bases, calculated from the ETa estimated by MFAO methodology, and harvest machine-measured yield data. The sums of soybean evapotranspiration (ETa) estimated by MFAO methodology (sum ETa MFAO) were 361.5, 360.9 and 344.3 mm for central pivots 1, 2 and 3, respectively, while the average soybean yield was 4,042 kg ha^{-1}. These yield values were very close to the mean value of the region, which was 3,960 kg ha^{-1} [31], and the yield is considerably higher when compared to Brazilian mean values, which were 3,206 kg ha^{-1} in the 2018/19 season [68]. The WP values were very close for the three central pivots, with a mean value of 1.14 kg m^{-3} or 11.37 kg ha^{-1} mm^{-1}. In the southern Brazil region, the attainable water productivity found for soybeans was 9.1 kg ha^{-1} mm^{-1} [69]. In the USA western Corn Belt region, an estimated soybean attainable water productivity was 9.9 kg ha^{-1} mm^{-1} [70]. These references support our current results.

On the other hand, we found values higher than the values found by Alfonso et al. [71] in Balcarce, Argentina. These authors evaluated the water productivity in soybeans, following a cover crop in a humid environment, and the highest value found was 8.3 kg ha^{-1} mm^{-1}, while the mean of all treatments was 7.23. It is important to note that the WP can suffer considerable variations according to irrigation management. For example, Gajić et al. [72] worked with four irrigation treatments (full irrigation, 65% of full irrigation, 40% of full irrigation and non-irrigated) during three experimental seasons and verified that under 65% of full irrigation, the soybean WP was 1.74 kg m^{-3}, while under full irrigation, it was only 0.59 kg m^{-3}. These results highlight the importance of studies related to controlled deficit irrigation to increase water use efficiency in agriculture.

Conclusions

Precise information about the spatiotemporal variability of actual crop evapotranspiration (ETa) and crop coefficient (Kc) is crucial for water efficient management in the agriculture, which is the largest user of freshwater in the world. Remote sensing models has a lot potential to be used for this purpose. Thus, we used EEFlux, a METRIC version that operates on the Google Earth Engine (GEE) system, in commercial soybean cultivation in the municipality of São Desidério, State of Bahia, Brazil, to map within-field variability of soybean evapotranspiration and crop coefficients.

Due to the lack of measured ET data, EEFlux modeled data were not validated but only compared to ET estimates by the MFAO method, which is a verified and utilized method in Brazil. Nevertheless, our findings confirm that the EEFlux platform, an innovative and free tool for access spatiotemporal variability of ETa and Kc at global scale is very efficient to estimate the ETa and Kc on different growth stages of soybean crop. The comparison between daily ETa estimated by the MFAO method and EEFlux showed good agreement for the three central pivots, exhibiting a d-*index* of 0.85, 0.83 and 0.89 for pivots 1, 2 and 3, respectively, but there is a subtle underestimation of ETa in comparison to that of the MFAO. Regarding the K$_c$ of EEFlux, with the exception of phenological phase II, good concordance was verified between

the K_c values considered in the comparison. In addition, the average WP equal to 1.14 kg m^{-3} indicates that water is being used with high efficiency in the soybean fields in the study.

ETa and K_c EEFlux are free access and ready-to-use, which makes them excellent data sources for the scientific community and other professionals involved in remote sensing in agricultural fields. However, in this study, we verified an anomaly related to the pixel oversize and low values of ETa and K_c in comparison to those in the non-affected zones. Further studies are necessary to correctly identify this issue. Last, ETa is a very dynamic phenomenon that depends especially on crop development, water supply and climatic conditions. Thus, the acquisition of a minimal number of images evenly distributed over the growing season for the assessment of spatial variability is very important. In this study, the six images used were able to characterize the variability in irrigated soybean cultivation once they were well distributed within the phenological phases.

Supporting information

S1 Fig. Natural color (RGB 432), false color (RGB 543), actual crop evapotranspiration (ETa), and fraction of the reference evapotranspiration (ETrF) referring to the image of the Landsat 8 satellite of 2017/01/06 when the soybean was with 074 days after sowing. The natural color and false color images show that there are no problems in the soybean fields. Thus, this strengthens our hypothesis that the error verified in the ETa and ETrF of the EEFlux is a consequence of the processing of the gridded weather data required to their calibration and calculation.
(DOCX)

S2 Fig. Actual crop evapotranspiration (ETa) referring to the image of the Landsat 8 satellite of 2017/01/06 when the soybean was with 074 days after sowing. A large area around the central pivots studied was selected to demonstrate the EEFlux error. The area inside of the dashed line refers to the part considered affected.
(DOCX)

S3 Fig. Fraction of the reference evapotranspiration (ETrF) referring to the image of the Landsat 8 satellite of 2017/01/06 when the soybean was with 074 days after sowing. A large area around the central pivots studied was selected to demonstrate the EEFlux error. The area inside of the dashed line refers to the part considered affected.
(DOCX)

Author Contributions

Conceptualization: Luan Peroni Venancio, Fernando Coelho Eugenio.

Data curation: Fernando Coelho Eugenio.

Formal analysis: Luan Peroni Venancio, Fernando Coelho Eugenio.

Investigation: Robson Argolo dos Santos.

Methodology: Luan Peroni Venancio, Fernando Coelho Eugenio, Roberto Filgueiras, Robson Argolo dos Santos.

Software: Robson Argolo dos Santos, Wilian Rodrigues Ribeiro.

Supervision: Fernando França da Cunha, Everardo Chartuni Mantovani.

Validation: Luan Peroni Venancio, Roberto Filgueiras, Fernando França da Cunha.

Visualization: Luan Peroni Venancio, Roberto Filgueiras.

Writing – original draft: Luan Peroni Venancio, Fernando Coelho Eugenio, Roberto Filgueiras, Robson Argolo dos Santos, Wilian Rodrigues Ribeiro, Everardo Chartuni Mantovani.

Writing – review & editing: Luan Peroni Venancio, Fernando Coelho Eugenio, Roberto Filgueiras, Fernando França da Cunha, Everardo Chartuni Mantovani.

References

1. FAO (Food and Agriculture Organization of the United Nations). The Future of Food and Agriculture, Trends and Challenges. Food and Agriculture Organization of the United Nations. Rome, Italy: FAO; 2017. Available: http://www.fao.org/3/a-i6583e.pdf

2. Grosso C, Manoli G, Martello M, Chemin YH, Pons DH, Teatini P, et al. Mapping maize evapotranspiration at field scale using SEBAL: A comparison with the FAO method and soil-plant model simulations. Remote Sensing. 2018;10.https://doi.org/10.3390/rs10091452

3. FAO (Food and Agriculture Organization of the United Nations). AQUASTAT—FAO's Global Information System on Water and Agriculture. Rome, Italy; 2014. Available: http://www.fao.org/3/I9253EN/i9253en.pdf

4. Zhang K, Bosch-Serra AD, Boixadera J, Thompson AJ. Investigation of water dynamics and the effect of evapotranspiration on grain yield of rainfed wheat and barley under a mediterranean environment: A modelling approach. PLoS ONE. 2015;10.https://doi.org/10.1371/journal.pone.0131360

5. Kamali MI, Nazari R. Determination of maize water requirement using remote sensing data and SEBAL algorithm. Agricultural Water Management. 2018; 209: 197–205.https://doi.org/10.1016/j.agwat.2018.07.035

6. Allen RG, Pereira LS, Raes D, Smith M. Crop evapotranspiration: Guidelines for computing crop water requirements. FAO Irrigation and Drainage Paper No. 56. FAO. Rome, Italy; 1998. Available: http://www.fao.org/tempref/SD/Reserved/Agromet/PET/FAO_Irrigation_Drainage_Paper_56.pdf

7. Chang Y, Wang J, Qin D, Ding Y, Zhao Q, Liu F, et al. Methodological comparison of alpine meadow evapotranspiration on the Tibetan Plateau, China. PLoS ONE. 2017; 12: 1–20.https://doi.org/10.1371/journal.pone.0189059

8. Paço TA, Pôças I, Cunha M, Silvestre JC, Santos FL, Paredes P, et al. Evapotranspiration and crop coefficients for a super intensive olive orchard. An application of SIMDualKc and METRIC models using ground and satellite observations. Journal of Hydrology. 2014; 519: 2067–2080.https://doi.org/10.1016/j.jhydrol.2014.09.075

9. Allen RG, Tasumi M, Morse A, Trezza R, Wright JL, Bastiaanssen W, et al. Satellite-Based Energy Balance for Mapping Evapotranspiration With Internalized Calibration (METRIC)—Applications. Journal of Irrigation and Drainage Engineering. 2007; 133: 395–406.https://doi.org/10.1061/(ASCE)0733-9437(2007)133

10. Allen RG, Tasumi M, Trezza R. Satellite-based energy balance for mapping evapotranspiration with internalized calibration (METRIC)—Model. Journal of irrigation and drainage engineering. 2007; 133: 380–394.https://doi.org/10.1061/(ASCE)0733-9437(2007)133:4(380)

11. Liaqat UW, Choi M. Surface energy fluxes in the Northeast Asia ecosystem: SEBS and METRIC models using Landsat satellite images. Agricultural and Forest Meteorology. 2015; 214–215: 60–79.https://doi.org/10.1016/j.agrformet.2015.08.245

12. French AN, Hunsaker DJ, Thorp KR. Remote sensing of evapotranspiration over cotton using the TSEB and METRIC energy balance models. Remote Sensing of Environment. 2015; 158: 281–294.https://doi.org/10.1016/j.rse.2014.11.003

13. Zhou H, Zhao W zhi. Modeling soil water balance and irrigation strategies in a flood-irrigated wheat-maize rotation system. A case in dry climate, China. Agricultural Water Management. 2019; 221: 286–302.https://doi.org/10.1016/j.agwat.2019.05.011

14. Teixeira AHC. Determining regional actual evapotranspiration of irrigated crops and natural vegetation in the São Francisco river basin (Brazil) using remote sensing and Penman-Monteith equation. Remote Sensing. 2010; 2: 1287–1319.https://doi.org/10.3390/rs0251287

15. Filgueiras R, Mantovani EC, Althoff D, Ribeiro RB, Venancio LP, Dos Santos RA. Dynamics of actual crop evapotranspiration based in the comparative analysis of sebal and metric-eeflux. Irriga. 2019; 1: 72–80.https://doi.org/10.15809/irriga.2019v1n1p72-80

16. Foolad F, Blankenau P, Kilic A, Allen RG, Huntington JL, Erickson TA, et al. Comparison of the automatically calibrated google evapotranspiration application-EEFlux and the manually calibrated METRIC application. Preprints. 2018;2018070040. https://doi.org/10.20944/preprints201807.0040.v1

17. Costa J de O, José JV, Wolff W, de Oliveira NPR, Oliveira RC, Ribeiro NL, et al. Spatial variability quantification of maize water consumption based on Google EEflux tool. Agricultural Water Management. 2020; 232: 106037. https://doi.org/10.1016/j.agwat.2020.106037

18. Allen R, Morton C, Kamble B, Kilic A, Huntington J, Thau D, et al. EEFlux: A Landsat-based evapotranspiration mapping tool on the Google Earth Engine. 2015 ASABE / IA Irrigation symposium: emerging technologies for sustainable irrigation—a tribute to the career of terry howell, Sr Conference Proceedings. St. Joseph, MI: ASABE; 2015. pp. 1–11. https://doi.org/10.13031/irrig.20152143511

19. Allen R, Morton C, Kamble B, Kilic A, Huntington J, Thau D, et al. EEFlux: A Landsat-based Evapotranspiration mapping tool on the Google Earth Engine. American Society of Agricultural and Biological Engineers, IA Irrigation Symposium: Emerging Technologies for Sustainable Irrigation. St. Joseph, MI: ASABE; 2015. pp. 1–11. https://doi.org/10.13031/irrig.20152143511

20. Rouse JW, Hass RH, Schell JA, Deering DW. Monitoring vegetation systems in the great plains with ERTS. Third ERTS Symposium [S.l]. NASA; 1973. pp. 309–317.

21. Venancio LP, Filgueiras R, Santos RA dos, Santos JEO. Spatial dynamics of remote sensing variables in irrigate robusta coffee. INOVAGRI International Meeting. Fortaleza, Ceará: Inovagri; 2019. https://doi.org/10.1017/CBO9781107415324.004

22. Ayyad S, Al Zayed IS, Ha VTT, Ribbe L. The performance of satellite-based actual evapotranspiration products and the assessment of irrigation efficiency in Egypt. Water (Switzerland). 2019;11. https://doi.org/doi:10.3390/w11091913

23. Khan A, Stöckle CO, Nelson RL, Peters T, Adam JC, Lamb B, et al. Estimating biomass and yield using metric evapotranspiration and simple growth algorithms. Agronomy Journal. 2019; 111: 536–544. https://doi.org/doi:10.2134/agronj2018.04.0248

24. Campana PE, Zhang J, Yao T, Andersson S, Landelius T, Melton F, et al. Managing agricultural drought in Sweden using a novel spatially-explicit model from the perspective of water-food-energy nexus. Journal of Cleaner Production. 2018; 197: 1382–1393. https://doi.org/10.1016/j.jclepro.2018.06.096

25. Bhattarai N, Liu T. LandMOD ET mapper: A new matlab-based graphical user interface (GUI) for automated implementation of SEBAL and METRIC models in thermal imagery. Environmental Modelling and Software. 2019; 118: 76–82. https://doi.org/10.1016/j.envsoft.2019.04.007

26. Molden D, Oweis T, Steduto P, Bindraban P, Hanjra MA, Kijne J. Improving agricultural water productivity: Between optimism and caution. Agricultural Water Management. 2010; 97: 528–535. https://doi.org/10.1016/j.agwat.2009.03.023

27. Li C, Xiong Y, Cui Z, Huang Q, Xu X, Han W, et al. Effect of irrigation and fertilization regimes on grain yield, water and nitrogen productivity of mulching cultivated maize (Zea mays L.) in the Hetao Irrigation District of China. Agricultural Water Management. 2020; 232. https://doi.org/10.1016/j.agwat.2020.106065

28. Zhang J, Sun H, Zhao L, Zhang C, Yan H, Peng B, et al. Nectar secretion of RN-type cytoplasmic male sterility three lines in soybean [Glycine max (L.) Merr.]. Journal of Integrative Agriculture. 2018; 17: 1085–1092. https://doi.org/10.1016/S2095-3119(18)61910-0

29. Jin Y, He J, Turner NC, Du YL, Li FM. Water-conserving and biomass-allocation traits are associated with higher yields in modern cultivars compared to landraces of soybean [Glycine max (L.) Merr.] in rainfed water-limited environments. Environmental and Experimental Botany. 2019; 168: 103883. https://doi.org/10.1016/j.envexpbot.2019.103883

30. Battisti R, Sentelhas PC, Pascoalino JAL, Sako H, de Sá Dantas JP, Moraes MF. Soybean yield gap in the areas of yield contest in Brazil. International Journal of Plant Production. 2018; 12: 159–168. https://doi.org/10.1007/s42106-018-0016-0

31. AIBA (Association of Farmers and Irrigators of Bahia). Haverst yearbook for western BA 2017/18. Barreiras, BA, Brazil; 2019. Available: http://aiba.org.br/wp-content/uploads/2019/06/Anuário-2019-Inglês-Digital.pdf

32. Alvares CA, Stape JL, Sentelhas PC, De Moraes Gonçalves JL, Sparovek G. Köppen's climate classification map for Brazil. Meteorologische Zeitschrift. 2013; 22: 711–728. https://doi.org/10.1127/0941-2948/2013/0507

33. INMET (Brazilian National Institute of Meteorology). Brazilian Climatological Normals 1981–2010. Brasília, DF, Brazil: Brazilian National Institute of Meteorology; 2018. Available: http://www.inmet.gov.br/portal/normais_climatologicas/mobile/index.html#p=1

34. ANA (Agência Nacional de Águas). Levantamento da agricultura irrigada por pivôs centrais no Brasil. 2nd ed. Brasília, Brazil: Agência Nacional de Águas; 2019. Available: http://arquivos.ana.gov.br/imprensa/arquivos/ProjetoPivos.pdf. Portuguese.

35. AIBA (Association of Farmers and Irrigators of Bahia). Agricultural yearbook of western Bahia region—Crop 2016/2017. Barreiras, BA, Brazil.; 2017. Available: http://aiba.org.br/wp-content/uploads/2019/06/Anuário-2019-Inglês-Digital.pdf

36. Mantovani EC, Bernardo S, Palaretti LF. Irrigação Principios e Métodos. 1st ed. Viçosa, MG, Brazil: Editora UFV; 2006. Portuguese.

37. Bernardo S, Mantovani EC, Silva DD, Soares AA. Manual de Irrigação. 9th ed. Viçosa, MG, Brazil: Editora UFV; 2019. Portuguese.

38. IRRIGER (Irrigation management and engineering). IRRIGER about us. 2020 [cited 1 Jul 2019]. Available: http://www.irriger.com.br/en-US/

39. Lima ALB, Filgueiras R, Mantovani EC, Althoff D, Santos RA dos, Venancio LP. Biophysical parameters and actual evapotranspiration of bean culture by means of remote sensing. Journal of Agricultural Science. 2019; 11: 156.https://doi.org/10.5539/jas.v11n13p156

40. Venancio LP, Chartuni E, do Amaral CH, Michael C, Neale U, Gonçalves IZ, et al. Forecasting corn yield at the farm level in Brazil based on the FAO-66 approach and soil-adjusted vegetation index (SAVI). Agricultural Water Management. 2019; 225: 105779.https://doi.org/10.1016/j.agwat.2019.105779

41. Vicente MR, Mantovani EC, Fernandes ALT, Neves JCL, Figueredo EM, Delazari FT. Spacial distribution of fertigated coffee root system. Ciência e Agrotecnologia. 2017; 41: 72–80.https://doi.org/10.1590/1413-70542016411021316

42. Singh RK, Irmak A. Estimation of Crop Coefficients Using Satellite Remote Sensing. Journal of Irrigation and Drainage Engineering-Asce. 2009; 135: 597–608.https://doi.org/10.1061/(Asce)Ir.1943-4774.0000052

43. Yuan Z, Shen Y. Estimation of Agricultural Water Consumption from Meteorological and Yield Data: A case study of Hebei, North China. PLoS ONE. 2013; 8: 1–9.https://doi.org/10.1371/journal.pone.0058685

44. Keller J, Bliesner RD. Sprinkle and trickle irrigation. New York: Van Nostrand Reinold; 1990.

45. Allen R, Irmak A, Trezza R, Hendrickx JMH, Bastiaanssen W, Kjaersgaard J. Satellite-based ET estimation in agriculture using SEBAL and METRIC. Hydrological Processes. 2011; 25: 4011–4027.https://doi.org/10.1002/hyp.8408

46. Allen RG, Walter IA, Elliotr R, Howell TA, Intenfisu D, Jensen ME. The ASCE standardized reference evapotranspiration equation. American Society of Civil Engineers. 2005.https://doi.org/10.3406/arasi.1965.919

47. Singh RK, Irmak A. Estimation of crop coefficients using satellite remote sensing. Journal of Irrigation and Drainage Engineering. 2009; 135: 597–608.https://doi.org/10.1061/(ASCE)IR.1943-4774.0000052

48. Suyker AE, Verma SB. Evapotranspiration of irrigated and rainfed maize—soybean cropping systems. 2009; 149: 443–452. https://doi.org/doi:10.1016/j.agrformet.2008.09.010

49. Monteiro LA, Sentelhas PC. Calibration and testing of an agrometeorological model for the estimation of soybean yields in different Brazilian regions. Acta Scientiarum Agronomy. 2014; 36: 265.https://doi.org/10.4025/actasciagron.v36i3.17485

50. Zhong Y, Shangguan Z. Water consumption characteristics and water use efficiency of winter wheat under long-term nitrogen fertilization regimes in northwest China. PLoS ONE. 2014;9.https://doi.org/10.1371/journal.pone.0098850

51. Willmott CJ. On the validation of models. Physical Geography. 1981; 2: 184–194.https://doi.org/10.1080/02723646.1981.10642213

52. Desclaux D, Roumet P. Impact of drought stress on the phenology of two soybean (Glycine max L. Merr) cultivars. Field Crops Research. 1996; 46: 61–70.https://doi.org/10.1016/0378-4290(95)00086-0

53. Hanway J, Thompson H. How a soybean plant develops. Special Report. 62. Ames, Iowa, United States; 1967. Available: http://lib.dr.iastate.edu/specialreports/62

54. McWilliams DA, Berglund DR, Endres GJ. Soybean—Growth and Management Quick Guide. NDSU Extension Service, North Dakota State University. 2004; 1–8. Available: http://www.marchutletseeds.ca/uploads/soybeans_soybeanstages.pdf

55. González-Gómez L, Campos I, Calera A. Use of different temporal scales to monitor phenology and its relationship with temporal evolution of normalized difference vegetation index in wheat. Journal of Applied Remote Sensing. 2018; 12: 1.https://doi.org/10.1117/1.jrs.12.026010

56. Yagci AL, Di L, Deng M. The effect of corn-soybean rotation on the NDVI-based drought indicators: A case study in Iowa, USA, using vegetation condition index. GIScience and Remote Sensing. 2015; 52: 290–314.https://doi.org/10.1080/15481603.2015.1038427

57. Yang Z, Zhao H, Di L, Yu G. A comparison of vegetation indices for corn and soybean vegetation condition monitoring. International Geoscience and Remote Sensing Symposium. 2009; 4: IV-801–IV-804. https://doi.org/10.1109/IGARSS.2009.5417498

58. Esquerdo JCDM, Zullo J, Antunes JFG. Use of NDVI/AVHRR time-series profiles for soybean crop monitoring in Brazil. International Journal of Remote Sensing. 2011; 32: 3711–3727. https://doi.org/10.1080/01431161003764112

59. Oliveira TC de, Ferreira E, Dantas AAA, OliveiraI TC de, FerreiraI E, Dantas AAA. Temporal variation of normalized difference vegetation index (NDVI) and calculation of the crop coefficient (Kc) from NDVI in areas cultivated with irrigated soybean. Ciência Rural. 2016; 46: 1683–1688. https://doi.org/10.1590/0103-8478cr20150318

60. Setiyono TD, Weiss A, Specht JE, Cassman KG, Dobermann A. Leaf area index simulation in soybean grown under near-optimal conditions. Field Crops Research. 2008; 108: 82–92. https://doi.org/10.1016/j.fcr.2008.03.005

61. Richter GL, Zanon AJ, Streck NA, Guedes JVC, KrÄulich B, Da Rocha TSM, et al. Estimating leaf area of modern soybean cultivars by a non-destructive method. Bragantia. 2014; 73: 416–425. https://doi.org/10.1590/1678-4499.0179

62. Campos I, González-Gómez L, Villodre J, Calera M, Campoy J, Jiménez N, et al. Mapping within-field variability in wheat yield and biomass using remote sensing vegetation indices. Precision Agriculture. 2019; 20: 214–236. https://doi.org/10.1007/s11119-018-9596-z

63. Kamble B, Kilic A, Hubbard K. Estimating crop coefficients using remote sensing-based vegetation index. Remote Sensing. 2013; 5: 1588–1602. https://doi.org/10.3390/rs5041588

64. Alam MS, Lamb DW, Rahman MM. A refined method for rapidly determining the relationship between canopy NDVI and the pasture evapotranspiration coefficient. Computers and Electronics in Agriculture. 2018; 147: 12–17. https://doi.org/10.1016/j.compag.2018.02.008

65. Bausch WC, Neale CMU. Crop coefficients derived from reflected canopy radiation: a concept. Transactions of the ASAE. 1987; 30: 703–709.

66. Mutiibwa D, Irmak S. AVHRR-NDVI-based crop coefficients for analyzing long-term trends in evapotranspiration in relation to changing climate in the U.S. High Plains. Water Resources Research. 2013; 49: 231–244. https://doi.org/10.1029/2012WR012591

67. Campos I, Neale CMU, Suyker AE, Arkebauer TJ, Gonçalves IZ. Reflectance-based crop coefficients REDUX: For operational evapotranspiration estimates in the age of high producing hybrid varieties. Agricultural Water Management. 2017; 187: 140–153. https://doi.org/10.1016/j.agwat.2017.03.022

68. CONAB (Companhia Nacional de Abastecimento). Acompanhamento da safra brasileira de grãos. Brasília, DF, Brazil; 2020. Available: https://www.conab.gov.br/info-agro/safras/graos. Portuguese.

69. Zanon AJ, Streck NA, Grassini P. Climate and management factors influence Soybean yield potential in a subtropical environment. Agronomy Journal. 2016; 108: 1447–1454. https://doi.org/10.2134/agronj2015.0535

70. Grassini P, Torrion JA, Yang HS, Rees J, Andersen D, Cassman KG, et al. Soybean yield gaps and water productivity in the western U.S. Corn Belt. Field Crops Research. 2015; 179: 150–163. https://doi.org/10.1016/j.fcr.2015.04.015

71. Alfonso C, Barbieri PA, Hernández MD, Lewczuk NA, Martínez JP, Echarte MM, et al. Water productivity in soybean following a cover crop in a humid environment. Agricultural Water Management. 2020; 232: 106045. https://doi.org/10.1016/j.agwat.2020.106045

72. Gajić B, Kresović B, Tapanarova A, Životić L, Todorović M. Effect of irrigation regime on yield, harvest index and water productivity of soybean grown under different precipitation conditions in a temperate environment. Agricultural Water Management. 2018; 210: 224–231. https://doi.org/10.1016/j.agwat.2018.08.002